small NANO MICRO

Cancer therapy

# Antitumor Activity and Prolonged Survival by Carbon-Nanotube-Mediated Therapeutic siRNA Silencing in a Human Lung Xenograft Model

*Jennifer E. Podesta, Khuloud T. Al-Jamal, Maria A. Herrero, Bowen Tian, Hanene Ali-Boucetta, Vikas Hegde, Alberto Bianco, Maurizio Prato, and Kostas Kostarelos**

*Carbon nanotubes are novel nanomaterials that are thought to offer potential benefits to a variety of biomedical and clinical applications. In this study, the treatment of a human lung carcinoma model in vivo using siRNA sequences leading to cytotoxicity and cell death is carried out using either cationic liposomes (DOTAP:cholesterol) or amino-functionalized multi-walled carbon nanotubes (*MWNT-$NH_3^+$*). Validation for the most cytotoxic siRNA sequence using a panel of human carcinoma and murine cells reveals that the proprietary siTOX sequence is human specific and can lead to significant cytotoxic activities delivered both by liposome or* MWNT-$NH_3^+$ *in vitro. A comparative study using both types of vector indicates that only* MWNT-$NH_3^+$*:siRNA complexes administered intratumorally can elicit delayed tumor growth and increased survival of xenograft-bearing animals. siTOX delivery via the cationic* MWNT-$NH_3^+$ *is biologically active in vivo by triggering an apoptotic cascade, leading to extensive necrosis of the human tumor mass. This suggests that carbon-nanotube-mediated delivery of siRNA by intratumoral administration leads to successful and statistically significant suppression of tumor volume, followed by a concomitant prolongation of survival of human lung tumor-bearing animals. The direct comparison between carbon nanotubes and liposomes demonstrates the potential advantages offered by carbon nanotubes for the intracellular delivery of therapeutic agents in vivo. The present work may act as the impetus for further studies to explore the therapeutic capacity of chemically functionalized carbon nanotubes to deliver siRNA directly into the cytoplasm of target cells and achieve effective therapeutic silencing in various disease indications where local delivery is feasible or desirable.*

**Keywords:**
- cancer therapy
- carbon nanotubes
- gene therapy
- liposomes
- RNA interference

[*] J. E. Podesta, Dr. K. T. Al-Jamal, B. Tian, H. Ali-Boucetta, V. Hegde, Prof. K. Kostarelos
Nanomedicine Lab, Centre for Drug Delivery Research
The School of Pharmacy, University of London
London WC1N 1AX (UK)
E-mail: kostas.kostarelos@pharmacy.ac.uk

Dr. A. Bianco
CNRS, Institut de Biologie Moléculaire et Cellulaire
UPR 9021 Immunologie et Chimie Thérapeutiques
67000 Strasbourg (France)

Prof. M. Prato, Dr. M. A. Herrero
Dipartimento di Scienze Farmaceutiche
Università di Trieste 34127 Trieste (Italy)

DOI: 10.1002/smll.200801572

## 1. Introduction

RNA interference (RNAi) is a powerful sequence-specific, post-transcriptional mechanism for gene silencing[1,2] that has rapidly progressed from a molecular phenomenon observed in plants, nematodes, and flies into a clinically relevant therapeutic option.[3] Silencing of genes using small interfering siRNA occurs at the cell cytoplasm,[4] in that way offering a significant advantage over gene expression of plasmid DNA that has to be delivered very efficiently to the cell nucleus. This is also a considerable advantage towards development of effective, non-viral gene therapeutics, since fewer intracellular barriers have to be overcome in siRNA silencing to achieve biological activity.[5,6]

Currently there are several clinical trials investigating RNAi for various disease indications, all of which deliver naked siRNA, that is, in the absence of any delivery system.[3] Uptake of naked, unmodified nucleic acids by cells is inefficient and random, therefore progress in clinical siRNA therapeutics currently under development will depend in large part on designing delivery vehicles to facilitate cell uptake, protect the siRNA from nuclease degradation, and enable targeted delivery. The lack of specific delivery vehicles for siRNA is becoming increasingly important in the effort to achieve rapid clinical progress and a lot of research activity is currently invested in designing siRNA delivery systems.[7,8] Any delivery system that would achieve translocation of siRNA directly into the cytoplasm would offer a great advantage towards effective silencing.

Gene silencing by siRNA delivery can be achieved efficiently in vivo by hydrodynamic injection (i.e., large-volume, high-pressure tail vein injection) that has been shown to produce high uptake (>50% cells) of siRNA in the liver.[9] However this is not a method that would easily translate to the clinic. In fact, the two most advanced reported studies of in vivo RNAi today have used delivery systems and administered the vectors into the systemic blood circulation. Zimmermann et al.[10] intravenously delivered siRNA against ApoB complexed with a 'stable nucleic acid lipid particle' (SNALP) to reduce both serum cholesterol and LDL levels in non-human primates, while Heidel et al. showed that multiple intravenous administrations at escalating doses of siRNA delivered by transferrin (Tf)-targeted polycationic cyclodextrins in non-human primates can be tolerated.[11]

RNA interference is also being studied extensively for its application in cancer therapy. Oncogenes as well as genes involved in angiogenesis, apoptosis, metastasis, and chemotherapy resistance have all been proposed as promising targets.[12,13] Complexes between siRNA with cationic liposomes and polymers have been described and are currently developed for the treatment of a variety of cancer preclinical models. One of the first reports of liposomal delivery of siRNA against cancer was by Yano and co-workers, silencing the human oncogene Bcl-2 with cationic liposome:siRNA complexes both by i.v. administration in a model of liver metastasis and by intratumoral injection into PC-3 prostate tumor xenografts.[14] Almost at the same time, Liu et al. reported growth inhibition of an MCF-7 breast carcinoma xenograft by intratumoral injection of Lipofectamine 2000:siRNA (against Hdm2, a negative regulator of p53).[15] Using local administration, Nogawa et al.[16] targeted pololike kinase 1 (Plk-1) in an orthotopic model of bladder, treating mice by transurethral delivery of a cationic liposome (LIC-1) complex with the siRNA. Using systemic (i.v.) vector administration, Li et al.[17] have recently described a liposome-based system comprising cationic liposomes, a polycationic peptide (protamine), and carrier DNA for delivery of siRNA in a mouse model of lung metastasis. A combination of siRNA sequences for MDM2, c-myc, and VEGF was able to reduce the mass of lung metastasis and increase animal survival. Pirollo et al.[18] used (i.v.) anti-HER-2 siRNA in a cationic liposome targeted to anti-transferrin receptor by a single-chain antibody fragment. This study was able to demonstrate tumor growth inhibition in a prostate (PANC-1) xenograft model in combination with a conventional chemotherapeutic agent. Earlier, Santel et al.[19,20] developed a novel cationic liposome (AtuFECT01) for systemic delivery of siRNA and reported reduction in tumor growth by silencing CD31 to achieve anti-angiogenesis.

Successful delivery of siRNA has also been reported using cationic polymers. Iwaki et al.[21] treated a pancreatic xenograft by intratumoral injections of Par-2 (proteinase activated receptor 2) siRNA with 0.5% atelocollagen to reduce tumor growth. Very recently, Futami et al. silenced the human helicase RecQL1(upregulated in rapidly dividing cells) to induce mitotic catastrophe by intratumoral injection of polyethyleneimine (PEI):siRNA complexes into a lung-cancer xenograft resulting in reduced tumor progression.[22] In an alternative approach, Leng et al.[23] tested histidine/lysine branched polymers for their ability to deliver therapeutic siRNA via intratumoral injection. They were able to demonstrate that the HK polymer effectively delivered Raf-1 siRNA to breast carcinoma (MDA-MB-435) human xenograft tumors, leading to tumor growth inhibition. PEI:siRNA complexes have also been intravenously targeted to induce in vivo gene silencing in specific cell types. Schiffelers et al. incorporated a PEGylated RGD peptide ligand to target the tumor vasculature that resulted in tumor-specific uptake and reduced tumor angiogenesis and growth by silencing VEGFR2.[24] Urban-Klein et al. silenced HER-2 using a PEI:siRNA complex and demonstrated that intraperitoneal administration of the complex was able to significantly inhibit tumor growth in a SKOV-3 xenograft model of ovarian cancer.[25]

Most of the studies mentioned above use intratumoral or intravenous administration of cationic liposomes or polymeric molecules to deliver siRNA into tumor cells via endocytosis. Novel nanomaterials that will facilitate more effective delivery of siRNA into the tumor cell cytoplasm are also being explored and may offer an alternative. Covalently functionalized carbon nanotubes (*f*-CNTs) have demonstrated their capacity to translocate the plasma membrane and deliver plasmid DNA to achieve exogenous gene expression.[26-28] Complexes between siRNA and lipid-coated CNTs have been described to be uptaken by tumor and T cells in vitro.[29,30] More recently, *f*-CNTs and polymer-coated *f*-CNTs have reported binding of siRNA and delivery to cells.[31,32] Only a single, preliminary in vivo study has appeared to date using chemically functionalized single-walled carbon nanotubes

  

small NANO MICRO

(*f*-SWNTs) for the delivery of siRNA silencing the expression of telomerase reverse transcriptase (TERT) in a mouse tumor model (Lewis Lung Carcinoma; LLC).[33] However, no study has yet demonstrated the capacity of *f*-CNTs to deliver siRNA into human tumor xenograft models in vivo, lead to tumor growth inhibition, and prolong the survival of tumor-bearing animals.

In this work we set out to comparatively study the treatment of a human carcinoma xenograft model using the delivery of a proprietary toxic siRNA sequence (siTOX) complexed with either one of the most widely used cationic liposome delivery systems (DOTAP:cholesterol) or with functionalized multi-walled carbon nanotubes (*f*-MWNTs). A human lung carcinoma tumor model in nude mice was established and treated, based on the hypothesis that *f*-CNTs can be used to efficiently deliver siRNA directly to the cytoplasm and elicit a specific effect resulting in delayed tumor growth, thereby significantly increasing survival.

## 2. Results

The complexes between cationic *f*-MWNTs (MWNT-$NH_3^+$) and siRNA were first formed and characterized. Functionalization of the MWNT with ammonium functional groups is known to increase the dispersibility and individualization of CNT in aqueous solutions and this was also observed for the MWNT-$NH_3^+$ used in this study (Figure S1 of Supporting Information). The number of amino groups at the surface of the MWNT-$NH_3^+$ was determined to be 0.147 mmol per gram of material by thermogravimetric analysis (TGA) and the quantitative Kaiser test. Complexation of the siRNA with the MWNT-$NH_3^+$ was studied using agarose gel electrophoresis by increasing the mass/charge ratio between the two components (Figure 1a). A reduction in the amount of free siRNA that was able to migrate in the gel indicated that the migration of duplex siRNA was retarded as complexation with the MWNT-$NH_3^+$ occurred. Sharp decreases in the fluorescence intensity of the bands that corresponded to free (non-complexed) siRNA were observed in the lanes with the highest MWNT-$NH_3^+$:siRNA mass ratios (64:1 and 80:1). The complexes were further characterized structurally using transmission electron microscopy (TEM) and atomic force microscopy (AFM). Comparison of the complex structures at two mass/charge ratios (Figure 1b) shows that increasing the MWNT-$NH_3^+$:siRNA ratio increases the degree of complexation evidenced by the formation of electron-rich (dark) areas on the nanotube surface, due to the condensation of siRNA. The TEM analysis indicated that complexation leads to more than one MWNT-$NH_3^+$ per complex. High-magnification TEM and AFM images (Figure 1c) showed that the surface of MWNT-$NH_3^+$ can be 'coated' with a layer of siRNA, which suggests surface interactions between the two oppositely charged components even at the MWNT-$NH_3^+$:siRNA 8:1 mass ratio. Because of this observed interaction, we hypothesized that at this low 8:1 mass ratio, siRNA could still be delivered efficiently by the MWNT-$NH_3^+$ and also minimize siRNA dose (concentration) and the possibility for off-target effects. This mass ratio was therefore selected to perform further biological studies.

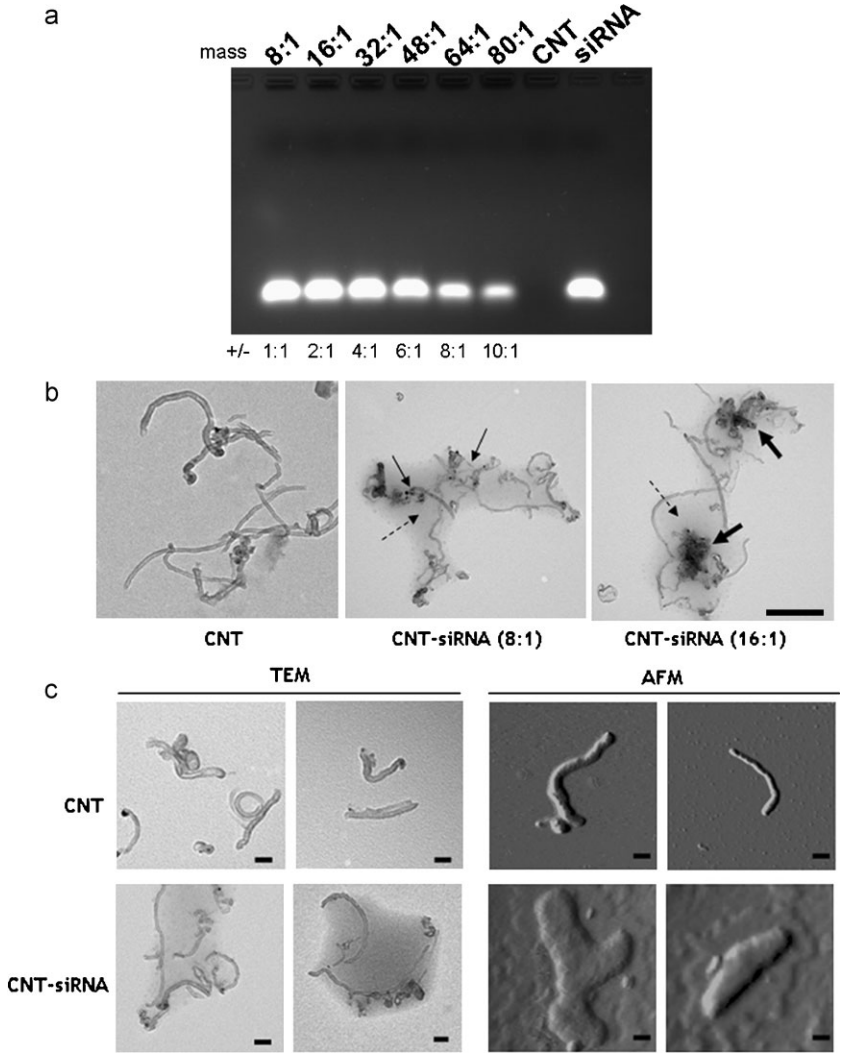


**Figure 1.** A) Electrophoretic mobility of siRNA complexed with MWNT-$NH_3^+$. Complexes were formed using 0.5 μg siRNA at different MWNT-$NH_3^+$:siRNA mass ratios: 8:1, 16:1, 32:1, 48:1, 64:1, and 80:1. Corresponding charge ratios are given for each complex. Mock-complexed siRNA and MWNT-$NH_3^+$ corresponding to the highest concentration used were run for comparison. siRNA was visualized by EtBr staining. B) TEM images of free MWNT-$NH_3^+$ and MWNT-$NH_3^+$:siRNA complexes formed at 8:1 and 16:1 mass ratios, at 250 μg $mL^{-1}$ final MWNT-$NH_3^+$ concentration. Scale bar is 500 nm. C) High-magnification TEM images and AFM amplitude images of MWNT-$NH_3^+$ (top panel) and MWNT-$NH_3^+$:siRNA complexes at 8:1 mass ratio (bottom panel). Final MWNT-$NH_3^+$ concentration is 250 μg $mL^{-1}$ or 50 μg $mL^{-1}$ for TEM or AFM, respectively. Scale bars 100 nm in all panels.

RNA interference using double-stranded siRNA has previously been demonstrated for many genes; however its efficacy still requires optimization for each sequence used to ensure the maximum silencing effect with the minimum off-target effects and toxicity from high doses of siRNA or cationic molecules used for delivery. In this study, the functional silencing capacity of the proprietary cytotoxic sequence siTOX was validated using one of the most widely used cationic liposome transfection agents that consisted of DOTAP:cholesterol (DOTAP:Chol, 2:1 molar ratio; Figure S2 of Supporting Information). The electophoretic mobility assay was used to identify the formation of liposome:siRNA complexes (Figure S2a) across a range of charge ratios from 1-8:1 (phospholipid nitrogen (N):siRNA phosphate (P)). Naked siRNA and liposomes alone corresponding to the highest amount for complexation (33 μg) were also run for comparison. In the lowest charge ratios (less than 2.5:1) free siRNA migrated identically to naked siRNA, indicating that the presence of the cationic liposome in the well does not interfere with electrophoresis. The gel was intentionally overexposed to reveal that complete complexation of all siRNA by the liposomes was obtained at charge ratios above 3:1 (N/P). The physicochemical characteristics of the liposome:siRNA complexes were also determined by dynamic light scattering, indicating that their mean diameter (184 nm) was larger than the one obtained for liposomes alone (147 nm) but with a much narrower size distribution and similar cationic surface charge (40.5 mV compared to 42.9 mV for the liposomes alone) (Figure S2b). The biological activity of the liposome:siRNA vectors was then studied for two doses of siRNA. In vitro silencing efficacy (Figure S2c) was determined in A549 (human lung carcinoma) cells using a final concentration of 20 or 80 nM siTOX, complexed with DOTAP:Chol over a range of charge ratios (1-8:1 N/P). siTOX is a toxic siRNA sequence that induces cell death; therefore the degree of cytotoxicity was considered an indication of silencing as determined by the MTT cell viability assay. Both concentrations of siRNA (20 and 80 nM) produced a dose response when used at increasing charge ratios up to N/P 4:1 and 8:1 at 80 and 20 nM, respectively. The 20 nM dose, however, produced a maximum of only 25% cell death when assayed after 72 h. Maximum cytotoxicity was obtained in cells treated with 80 nM siRNA complexed at 4:1 N/P (>50%), and this combination was taken further for additional in vitro validation.

In order to demonstrate the specificity of siTOX against human carcinomas, a panel of human and mouse cell lines were screened for their susceptibility to siTOX transfected with DOTAP:Chol at the optimized conditions of N/P 4 and 80 nM (Figure S3 of Supporting Information). Treatment of all human cell lines (Figure S3a) resulted in significant cell death in the liposome:siTOX treated groups compared to the control groups. A sequence designed against the pololike kinase 1 (*PLK-1*) gene was used as a positive control. PLK-1 is known to play a role in cell cycle progression and is critical for progression from G2-M phase.[34] Silencing PLK-1 prevents mitosis and induces apoptosis and has been previously used in therapeutic silencing experiments.[16] A non-coding (siNEG) sequence was used as a negative control and did not cause significant cell death. The MTT assay results showed that siTOX generally had high specificity for human cancer cells with all cell lines showing significant toxicity ($p < 0.001$) compared with the control groups. The murine cells (Figure S3b) were considerably less sensitive to both apoptosis-inducing siRNAs, indicating the specificity of siTOX for human cells. Based on this data, human lung carcinoma (Calu 6) cells were shown to be susceptible to siTOX treatment and were further used to establish human carcinoma xenograft models.

Silencing leading to cytotoxicity using carbon nanotubes as a delivery system was considerably more difficult to be quantitatively determined using the MTT assay. There have been numerous published reports that CNT interfere with most colorimetric assays used to determine cytotoxicity leading to unreliable data that should be treated with caution.[35,36] In order to determine the in vitro efficacy of the MWNT-$NH_3^+$:siRNA complexes, we compared optical microscope images of the transfected cell cultures that did not suffer from such handicaps (Figure S4 of Supporting Information). Photomicrographs representative of at least 6 independent wells were compared for the human lung carcinoma (Calu 6) cells receiving different treatments. Cells were treated with MWNT-$NH_3^+$:siRNA complexes prepared at 8:1 and 16:1 mass ratios and the optimized liposome:siRNA complex was included as a positive control (80 nM; N/P = 4). Cell death in wells treated with MWNT-$NH_3^+$:siRNA at both mass ratios was observed by the presence of fewer cells compared to the MWNT-$NH_3^+$:siNEG and MWNT-$NH_3^+$ alone controls. Interestingly, the liposome:siRNA treated cells did not show cell death at the 24 h time point (as determined by optical microscopy); however, when the MTT assay (Figure S3) was performed 72 h post transfection, cytotoxicity was evident in approximately 50% of the cell population. The induction of cell death occurred at a much earlier time point in cells treated with *f*-CNTs versus liposomes in the course of the present study and in multiple cell culture experiments. More experimentation is needed to determine the dynamics of siRNA delivery, intracellular trafficking and activity by *f*-CNT-mediated delivery compared to liposomal delivery.

To test the efficacy of the vectors in vivo, human tumor xenografts (Calu 6) were grown subcutaneously. When tumor volume reached an average of 300 $mm^3$, 50 μL of the vector dispersion was injected longitudinally within the tumor mass. MWNT – $NH_3^+$:siTOX and MWNT – $NH_3^+$:siNEG at 8:1 mass ratio, MWNT – $NH_3^+$ alone and siTOX alone (Figure 2a, right panel) were slowly injected intratumorally. Liposome groups (Figure 2a, left panel) were treated with liposome:siTOX, liposome:siNEG and liposome alone. MWNT – $NH_3^+$:siTOX significantly inhibited tumor growth as compared to naïve (5% dextrose treated animals) and MWNT – $NH_3^+$:siNEG. Tumor growth was noticeably inhibited following the second therapeutic dose, which suggested that the dosing regime is crucial in order to effectively maintain gene silencing. By day 27, MWNT – $NH_3^+$:siTOX had inhibited tumor growth significantly as compared to siTOX and MWNT – $NH_3^+$ alone groups. In the liposome-treated groups, no significant effect on tumor growth from intratumoral administrations of the liposome:siTOX was obtained compared to control-treated

  

small NANO MICRO

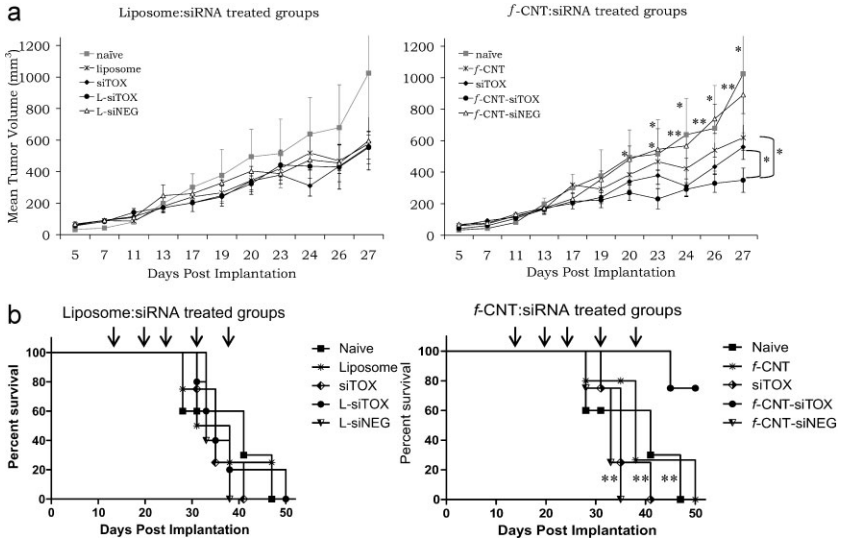


**Figure 2.** Tumor growth and survival curves after intratumoral administration of *f*-CNT:siTOX and liposome:siTOX complexes in Calu 6 xenografts. A) Growth curves of human xenograft tumors. Calu 6 cells were inoculated under the skin of nude mice and intratumoral injection of siTOX began when mean tumor volume reached 300 $mm^3$. siRNA (4 μg) was complexed with either *f*-CNT (8:1 mass ratio) or DOTAP:Chol liposomes (4:1 N/P). Non-coding siRNA (siNEG) was similarly injected as a negative control and each component (liposome, CNT, siTOX) was injected individually. 50 μL of sterile, 5% dextrose was injected into naïve animals. *p* values = *<0.05; **<0.01. *f*-CNT-siTOX to naïve: $p < 0.05$ (from day 23); *f*-CNT-siTOX to *f*-CNT-siNEG: $p < 0.05$ (from day 20); *f*-CNT-siTOX to *f*-CNT alone: $p < 0.05$ (day 27); *f*-CNT-siTOX to siTOX: $p < 0.05$ (day 27); no significance for liposome treated groups; each group $n = 4–6$, error bars: ±s.e.m. B) Survival analysis of Calu 6 xenograft mice. Mice were intratumorally injected with 50 μL liposome-siRNA formulations (left) or *f*-CNT:siRNA vectors (right); naïve (5% dextrose); DOTAP:Chol (2:1 molar ratio); siTOX (4 μg); Liposome:siTOX (N/P = 4; 4 μg siRNA); Liposome:siNEG (N/P = 4; 4 μg siRNA); *f*-CNT (32 μg); *f*-CNT:siTOX (mass ratio = 8:1; 4 μg siRNA); *f*-CNT:siNEG (mass ratio = 4:1; 4 μg siRNA).**$p < 0.01$ for *f*-CNT-siTOX as compared to naïve, *f*-CNT-siNEG and siTOX alone groups. No significance for liposome treated groups; $n = 4–6$.

groups. The effect of MWNT – $NH_3^+$:siTOX on inhibition of tumor volume and growth arrest after 27 days, the time point at which control groups reached maximum permitted volume, was statistically significant compared to the liposome:siTOX group. On day 50 after tumor implantation the therapeutic outcome of a total of five administrations (day 14, 20, 24, 31, 38) was analyzed in terms of animal survival (Figure 2b) for the liposome-treated (Figure 2b, left panel) and the MWNT – $NH_3^+$ treated groups (Figure 2b, right panel). Animals in the MWNT – $NH_3^+$:siTOX treated group demonstrated tumor growth inhibition, which resulted in significant increase in survival compared to naïve, MWNT – $NH_3^+$:siNEG and siTOX alone. There was no significant increase in survival seen in animals treated using cationic liposomes to deliver siTOX.

Tumors that received the therapeutic MWNT-$NH_3^+$:siTOX complexes began to show signs of collapse that did not appear to be size dependent (such an effect was not observed in equivalent-sized tumors in control groups) nor should they be attributed to MWNT-$NH_3^+$ cytotoxicity. In order to investigate the mechanism behind the observed tumor-volume collapse and the ensuing benefit in survival for the MWNT-$NH_3^+$:siTOX treated animals, tumors from all groups were excised and sectioned when the maximum allowed tumor volume of 800–1000 $mm^3$ was reached (Figure 3). The top panel in Figure 3 shows photographs of the cross-sectioned tumors from each group. Tumors treated with MWNT-$NH_3^+$ alone showed nanotube accumulation along the injection needle tracks. Tumors from the MWNT-$NH_3^+$:siTOX group either collapsed, resulting in a lesion at the surface of the tumor or, as in the tumor shown, complete collapse of tissue at the tumor core. The fluid at the tumor core was gray colored in all tumors in that group, indicating the presence of CNT without any observed inflammation. Heamatoxylin/eosin (H&E) staining of the sectioned tumor tissues revealed extended necrosis in the areas around the nanotubes only in the case of the MWNT-$NH_3^+$:siTOX group. Viable tissue was found in all tumor sections for all other treated groups, including the MWNT-$NH_3^+$ alone treated group (Figure 3, second row). Liposome:siTOX showed no significant tumor necrosis compared to naïve animals. TUNEL staining, which specifically incorporates fluorescein onto the ends of nicked DNA and is widely used as a marker for apoptosis, was used to stain sections of the tumor tissues (green channel) in contrast to propidium iodide (PI) counterstaining all nuclei (red channel; Figure 3, third row). Phase images (Figure 3, bottom row) corresponding to the TUNEL/PI stained sections indicated that cell death in the MWNT-$NH_3^+$:siTOX treated group correlated well with regions of nanotube accumulation. The equivalent regions in the tumor sections treated with MWNT-$NH_3^+$ alone did not correspond to apoptotic cells, which further suggested that the observed cytotoxicity is not due to MWNT-$NH_3^+$ toxic effects but to the activity of the MWNT-$NH_3^+$:siTOX vector. Naïve and liposome:siTOX treated groups both showed predominantly healthy cells (in red) with scarce areas of cells positive for apoptosis (in green) consistent with some degree of tissue necrosis that developed at the core of all tumors as the volume increased.

The intralesional delivery of siTOX by complexation with MWNT-$NH_3^+$ was the only treatment condition that resulted in statistically significant tumor growth inhibition, collapse of the tumor mass, and prolonged survival of the animals in that group. Moreover, the observed therapeutic benefit was found to be a result of extended tumor cell apoptosis and necrosis that correlated with the localization of the vectors only in the case of the MWNT-$NH_3^+$:siTOX complexes.

## 3. Discussion

In an effort to translate the powerful concept of gene silencing to clinical cancer therapeutics, the engineering of novel delivery systems that could achieve translocation of

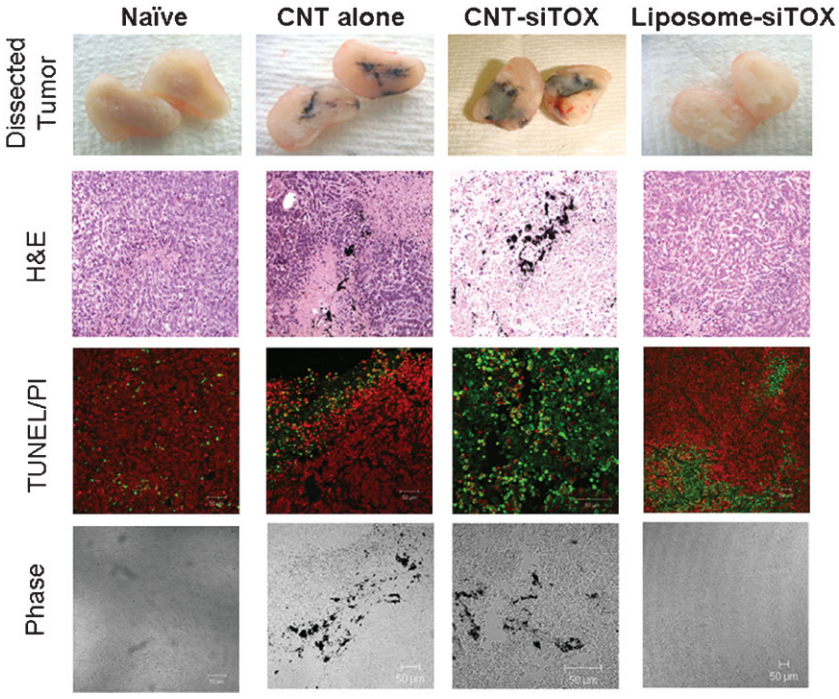


**Figure 3.** MWNT-$NH_3^+$:siTOX complexes induced tumor collapse and apoptosis of human Calu 6 xenograft tumors. Whole tumors were excised upon reaching 800–1000 $mm^3$ and photographed. Top-row images (left to right) are representative tumors from naïve, MWNT-$NH_3^+$ alone, MWNT-$NH_3^+$:siTOX, and liposome:siTOX groups. Tumors were then fixed in 10% buffered formalin, paraffin embedded, and sectioned. H&E staining was performed (second row) or sections were deparaffinised and rehydrated through graded ethanol then TUNEL and propidium iodide nuclear counterstain were used to identify apoptotic (green) cells from the total cell population (red, third row). Phase images of corresponding fields of view for TUNEL/PI are shown in the last row to indicate MWNT-$NH_3^+$ localization.

double-stranded siRNA directly into the tumor cell cytoplasm and effective silencing has become imperative. Carbon nanotubes offer the possibility for highly efficient cytoplasmic transport of siRNA based on their previously described capacity to translocate the plasma membrane even under conditions unfavorable to energy-dependent endocytosis.[38] In the present study, we have comparatively studied the in vivo cytotoxic activity of complexes between a toxic siRNA sequence with either functionalized MWNTs or cationic liposomes (DOTAP:Chol). Such head-to-head comparative study of two different types of delivery system has not been previously carried out and is considered extremely important towards development and validation of novel nanomaterial-based delivery systems.

Complexes between cationic liposomes and double-stranded nucleic acids are established non-viral vectors that have already been studied clinically for a variety of disease indications (of the liver, lung, or cancer), primarily using plasmid DNA.[39,40] Cationic liposomes are also under development for the delivery of therapeutic siRNA against hepatic and oncology indications.[41,42] DOTAP:Chol was selected in the present study as one of the most thoroughly studied cationic liposome systems for both systemic and intratumoral administration.[43,44] Also, DOTAP:Chol liposomes served as an in vitro siRNA transfection agent used to validate the biological (cytotoxic) activity of the proprietary siRNA sequence siTOX. Complexes between liposomes and siTOX were formed by electrostatic interaction at various charge ratios (Figure S2), in agreement with previously described cationic liposome:siRNA (and pDNA) complex formation studies and were used as such throughout this study.[45,46]

The use of siRNA to induce cell death by silencing genes involved in apoptotic cascades has been explored extensively in vitro. Several gene targets have been silenced by siRNA and mixed results have been obtained; however, it has provided very useful information on the molecular mechanism and specific pathways of apoptosis.[47] The use of siRNA towards promoting apoptosis was first explored by Yano et al.[14] silencing Bcl-2 due to its high level of expression in the tumor microenvironment and the significant role it plays in regulating the mitochondrial-mediated apoptotic pathway.[48] The delivery of siRNA sequences triggering cytotoxicity to achieve tumor elimination is still primarily used in combination with conventional anti-cancer therapeutic agents with an aim to improve sensitivity and overcome chemotherapy resistance.[49] The cytotoxic siTOX sequence in this study has been previously used only in vitro as an indicator of transfection efficiency.[50] Validation of the siTOX sequence was carried out in this study using DOTAP:Chol liposomes and a panel of human and murine cell lines (Figure S3 of Supporting Information). Specificity for all human tumor cell lines was evidenced by the dramatic enhancement of cytotoxicity (Figure S3a) compared to that obtained for the panel of murine cells (Figure S3b). Based on that data, Calu 6 (human lung carcinoma) cells were selected to establish human tumor xenografts and comparatively study the in vivo cytotoxic activity of siTOX delivered by either liposomes or MWNT-$NH_3^+$. Previously, Calu 6 cells have been used extensively in human xenograft models of NSCLC to test treatment by small-molecule inhibitors of tyrosine kinases.[37,51]

Complexation between *f*-SWNTs and nucleic acids was first described for $\beta$-gal encoding plasmid DNA.[26] Complex formation was then shown to be achieved by both *f*-SWNT and *f*-MWNT that moderately enhanced gene expression in mammalian cells compared to naked plasmid DNA.[27] To date, a variety of different types of carbon nanotubes have been shown to be able to deliver nucleic acids.[52] Here, complexes between the positively charged MWNT-$NH_3^+$ and siTOX were formed and characterized by electron and atomic force microscopy (Figure 1). Complexation of siRNA occurred at the surface of MWNT-$NH_3^+$ even at low charge ratios evidenced as a high electron density (TEM), thick (AFM) coat around the MWNT-$NH_3^+$ (Figure 1c). Complexes between carbon nanotubes and siRNA have been reported

  

previously[29,32,33,53–55] but detailed structural characterization of such complexes is still lacking. More biophysical work is warranted to elucidate the interactions between the short (19–23 mer), double-stranded siRNA sequences, and CNTs that should be significantly different to the much more thoroughly characterized complexes between CNTs and single- or double-stranded DNA.

The biological (cytotoxic) activity of the MWNT-$NH_3^+$:siTOX complexes were initially evaluated in vitro using Calu 6 cell cultures (Figure S3). Enhanced cytotoxicity was observed in the case of the MWNT-$NH_3^+$:siTOX complexes (at both charge ratios used) and in comparison to either a scrambled (non-cytotoxic) siRNA sequence and that of liposome:siTOX complexes. Interestingly, the liposome: siTOX complexes were shown to achieve maximum biological activity at 72 h post-transfection (Figure S3a), leading up to 50% Calu 6 cell kill. In contrast, the MWNT-$NH_3^+$:siRNA complexes reached optimum activity at an earlier time point after transfection (24 h). This suggested that MWNT– $NH_3^+$:siRNA may be reaching the cytoplasm more rapidly than liposome:siRNA leading to faster cell kill, further supporting the hypothesis that *f*-CNTs can translocate through the plasma membrane more readily. However, more intracellular trafficking experimental evidence is needed to verify this observation.

Intratumoral administration of siRNA has been previously reported in vivo for both liposome:siRNA and MWNT-$NH_3^+$:siRNA.[22,33] Even though intralesional administration of therapeutics is by no means optimal for clinical cancer treatment, it offers a way to achieve high doses of biologically active substances locally at the tumor site. Moreover, the only clinically used gene therapy pharmaceutical is a recombinant human adenovirus-p53 (Gendicine), which has received approval by the SFDA for intratumoral treatment of head and neck carcinoma patients.[56] There are also significant advances made in image-guided techniques and protocols that will allow more accurate and effective intralesional administration into deep-seated tumors. Previous intratumoral administration of complexed siRNA towards therapeutic treatment of cancer has shown encouraging results. Several branched histidine/lysine (HK) polymers were synthesized and screened for the ability to deliver functional siRNA. Targeting Raf-1 in MDA-MB-43 human xenograft resulted in 50% reduction in tumor volume as well as inducing apoptosis.[57,58] Tumor angiogenesis was also affected, as evidenced by a reduction in blood-vessel density. Leng et al. have gone on to optimize the HK:siRNA complexes for systemic delivery,[23] thus demonstrating the need for intratumoral administration, not only as a potential therapeutic route but also as a stage in the clinical development of novel gene therapeutics. More recently, Kim et al.[59] have evaluated polyelectrolyte complex micelles for the delivery of VEGF siRNA both intratumorally and intravenously. Interestingly, the intratumoral administration of liposome-based siRNA complexes, consistent with the findings of this study, underperforms when compared to other routes of administration such as intravenous or intraperitoneal.

In the present study, a siTOX dose of 4 μg was complexed with cationic liposomes or MWNT-$NH_3^+$ then administered by intratumoral injection into Calu 6 xenograft tumors. Complete complexation of siRNA at 4:1 N/P with liposomes was demonstrated (Figure S2a) by agarose gel electrophoresis. The interaction between MWNT-$NH_3^+$:siRNA at the 8:1 mass ratio used in biological experiments as observed by TEM (Figure 1b) indicated the association of nucleic acids with the MWNT-$NH_3^+$ surface even though complete condensation of the siRNA was not obtained by agarose gel electrophoresis at this mass ratio (Figure 1a). We decided to study the 8:1 mass ratio complexes in order to minimize the siRNA dose and reduce the possibility for off-target effects. Treatment led to statistically significant reduction in tumor volume only in the case of MWNT-$NH_3^+$:siRNA complexes (Figure 2a). More importantly, the reduction in mean tumor volume was translated to prolonged animal survival only for the MWNT – $NH_3^+$:siTOX after 50 days post Calu 6 xenograft implantation (Figure 2b). Prolonged survival of tumor-bearing animals has not been previously reported for any kind of therapeutic modality by using any type of CNT. The only previous study using a different type of CNT (carboxylated and converted to amino-functionalised SWNT) complexed to siRNA silencing mTERT, reported only some reduction of the tumor volume for the *f*-SWNT:siRNA-treated animals after intratumoral administration of the complexes.[33] The animal model used was a syngeneic (C57BL/6) murine model (LLC) in contrast to the human lung xenograft model used in this study.

Gross examination of the treated tumor lesions indicated that administration of the MWNT-$NH_3^+$:siRNA complexes was leading to tumor collapse from the inside of the tumor. This indicated that siTOX activity was occurring locally at the site of injection leading to collapse of the tumor mass (top panel, Figure 3). Histological examination and TUNEL/PI staining for apoptosis of the treated tumor lesions indicated that in the case of MWNT – $NH_3^+$ alone injections, clusters of nanotubes could be observed within the tumor mass surrounded predominantly by healthy, non-apoptotic tumor cells. In the case of MWNT-$NH_3^+$:siTOX injections, nanotube accumulation was always co-localized within necrotic regions, that under the TUNEL/PI assay indicated extensive apoptosis-positive cells. More tissues (lung, liver, spleen and kidneys) were also dissected and examined histologically but no CNTs were observed in any of these tissues (data not shown). Liposome:siTOX intratumoral injections did not indicate neither significant necrosis nor apoptosis under identical experimental conditions.

Overall, this data indicated that siTOX delivery via cationic MWNT-$NH_3^+$ was biologically active by triggering an apoptotic cascade leading to extensive necrosis of the human tumor cells. This suggests that therapeutic silencing by delivery of toxic siRNA sequences can be considered an effective cancer therapeutic. Carbon-nanotube-mediated delivery of siRNA by intratumoral administration has hereby been shown to lead to successful and statistically significant suppression of tumor volume, followed by a concomitant prolongation of survival of human lung tumor-bearing animals. Such observations become more significant in view of the experimental design followed in this study, since the direct comparison between carbon nanotubes and liposomes demonstrated the potential advantages offered by carbon

nanotubes for the intracellular delivery of therapeutic modalities in vivo. The data obtained in this study further illustrate the capacity of *f*-CNT to translocate the plasma membrane much more efficiently compared to more established delivery systems (such as cationic liposomes) in the case of local administration directly at the disease site to achieve advantages in therapeutic activity. The present work can act as the impetus for further studies to explore the therapeutic capacity of chemically functionalized carbon nanotubes to deliver siRNA into the cytoplasm of target cells to achieve effective therapeutic silencing of various disease indications where local delivery is feasible or desirable.

## 4. Experimental Section

The proprietary sequence siCONTROL TOX (referred to throughout this manuscript as siTOX) and custom synthesized PLK-1 siRNA were purchased from Dharmacon (Lafayette, CO, USA). Non-coding siNEG was purchased from Eurogentec (UK). siPlk-1 sequence is 5′- CCUUGAUGAAGAAGAUCACdTdT-3′.

1,2-dioleoyl-3-trimethylammonium-propane (chloride salt) (DOTAP, 99%) and cholesterol were purchased from Avanti Polar Lipid (USA); 0.1 μm and 0.2 μm filter from Millipore (UK); DeadEnd Fluorometric TUNEL System was from Promega (UK). MTT (3-(4,5-dimethylthiazol-2-yl)-2,5-diphenyltetrazolium bromide), dimethyl sulfoxide (DMSO), chloroform and methanol from Sigma (UK); Diethyl pyrocarbonate (Sigma, UK) (DEPC)-treated water was used in all preparations (0.1% DEPC treatment overnight, followed by autoclaving). Dulbecco's modified Eagle medium (DMEM), Advanced RPMI, minimum essential medium (MEM), fetal bovine serum (FBS), penicillin/streptomycin, and phosphate buffered saline (PBS) from Gibco, Invitrogen (UK).

Human lung carcinoma Calu 6 and murine vascular endothelial cells SVEC 4-10 and 2F2B were a kind gift from AstraZeneca, UK. Human lung carcinoma A549 (CCL-185); human breast carcinoma MCF-7 (HTB-22); human prostate carcinoma cell lines DU145 (HTB-81) and C-33 A (HTB-31) human embryonic kidney (HEK) 293 (CRL-1593); human cervical cancer cell line HeLa (CCL-2.2); Murine melanoma B16F10 (CRL-6475); and fibroblast cells NIH 3T3 (CRL-1658) from ATCC (UK).

Liposomes were prepared by lipid film hydration method followed by filtration. Briefly, DOTAP and cholesterol (2:1 molar ratio) were dissolved in chloroform:methanol (4:1 v/v), the organic solvent was evaporated in a rotary evaporator (Buchi, Switzerland) under vacuum at 40 °C for 30 min and then flushed with a $N_2$ stream to remove any residual traces of organic solvent. The dried lipid film was hydrated with 1 ml of 5% dextrose, sonicated and extruded twice through a 0.1-μm filter under sterile conditions. The final lipid concentration was 2mM.

MWNTs were purchased from Nanostructured and Amorphous Materials Inc. (Houston, TX; Lot # 1240XH, 95%). Outer average diameter was 20–30 nm, and length between 0.5–2 μm. *f*-MWNTs were prepared following the 1,3 dipolar cycloaddition reaction as previously described.[60,61] Ammonium-functionalized multi-walled carbon nanotubes (MWNT-$NH_3^+$) were dispersed in 10% dextrose or deionized water at a concentration of 1–1.3 mg $mL^{-1}$. The dispersion was sonicated for 15 min at room temperature in a bath sonicator (Ultrasonic cleaner, VWR) before each use and stored at 4 °C until further use.

*Electrophoretic mobility shift assay:* Complexes were prepared by mixing 0.5 μg siRNA (30 μL) with DOTAP:Chol liposomes at different charge ratios or with MWNT-$NH_3^+$ at different mass ratios. Complexes were incubated at room temperature for 30 min to allow complete formation before loading onto 1% agarose/TBE gel containing ethidium bromide (0.5 μg $mL^{-1}$). Naked siRNA (0.5 μg), MWNT-$NH_3^+$ and liposome alone were included for comparison. The gel was run for 45 min at 70 V and visualized under UV light using GeneGenius system, PerkinElmer Life and Analytical Sciences (USA).

*TEM:* MWNT-$NH_3^+$ (15 μL of 0.5 mg $mL^{-1}$ in 10% dextrose) was complexed with an equal volume of siRNA at 8:1 and 16:1 MWNT-$NH_3^+$:siRNA mass ratios. The complex was left to equilibrate for 30 min. A drop of the suspension was placed on a grid with a support film of Formvar/carbon, excess material was blotted off with a filter paper and the complexes were examined, without being negatively stained, under a FEI CM120 BioTwin transmission electron microscope (Einhoven, Netherlands) using a Lab6 emitter. Images were captured using an AMT Digital Camera.

*AFM:* MWNT-$NH_3^+$ (15 μL of 0.1 mg $mL^{-1}$ in water) were complexed with an equal volume of siRNA at 8:1 MWNT-$NH_3^+$:siRNA mass ratios. The complex was left to equilibrate for 30 min. Approximately 20 μL of siRNA, MWNT-$NH_3^+$ or the complex was deposited on the surface of freshly cleaved mica (Agar Scientific, Essex, UK), allowed to adsorb for 5 min. Unbound structures were removed by washing with 0.22-μm filtered deionized $H_2O$, then dried under a nitrogen stream. Imaging was carried out in TappingMode using a Multimode AFM, E-type scanner, Nanoscope IV controller, Nanoscope 5.12b control software (Veeco, Cambridge, UK) and a silicon tapping tip, made of crystallized silicon (NSG01, NTI-Europe, Apeldoorn, The Netherlands) of curvature radius of 10 nm. The tip was mounted on tapping-mode silicon cantilever with a typical resonant frequency of 150 kHz and a force constant of 5.5 N/m, to image 5 μm × 5 μm square areas of the mica surface, with a resolution of 512 × 512 pixels and a scan rate of 1 Hz. All AFM images were performed in air.

*Liposome:siRNA and MWNT-$NH_3^+$:siRNA complexation for biological studies:* siRNA complex preparation for in vivo experiments was carried out by diluting the appropriate volume of liposome (1.4 mg $mL^{-1}$) or MWNT-$NH_3^+$ (1.28 mg $mL^{-1}$) dispersion to a total volume of 25 μL in 5% dextrose, to achieve liposome:siRNA N/P = 4 or MWNT-$NH_3^+$:siRNA mass ratio = 8. An equal volume of 160 μg $mL^{-1}$ siRNA in 5% dextrose was then added to the liposome or MWNT-$NH_3^+$ aliquots and mixed by rapid pipetting, yielding a final siRNA concentration of 80 μg $mL^{-1}$. 50 μL of the complex was injected per animal. A similar procedure was used to prepare complexes for in vitro experiments except that complexation was carried out at siRNA concentration of 1.25 or 5μg $mL^{-1}$ then diluted 5× with culture media yielding siRNA final concentration of 20 or 80 nM, respectively.

*Cell cultures:* A549,HeLa, HEK 293, B16F10, SVEC 4-10, 2F2B and NIH 3T3 cells were maintained in DMEM; C33a and MCF-7 cells were maintained in MEM, and Calu 6 cells were maintained

  

in Advanced RPMI, all supplemented with 10% fetal bovine serum (FBS), 50 U $mL^{-1}$ penicillin, 50 μg $mL^{-1}$ streptomycin, 1% L-glutamine and 1% non-essential amino acids at 37 °C in 5% $CO_2$. Cells were passaged when they reached 80% confluence in order to maintain exponential growth. Calu 6 cells used for tumor inoculation were passaged two times in antibiotic-free media to ensure the line was free of contaminants prior to implantation.

*Transfection of human and murine cell lines with siRNA:* Cells (12 500 cells/well) were seeded into 96-well plates. 24 hours later, cells were transfected with an apoptosis inducing siRNA (siPlk1 or siTOX). Briefly, 30 μL of the pre-formed siRNA complex was diluted 5 times with serum free media and 150 μL of the complex containing media was added to each well yielding a final siRNA concentration of 20 or 80 nM. Four hours later, 150 μL of fresh media containing 20% FBS was added to each well. After 72 h incubation at 37 °C and 5% $CO_2$, MTT assay was performed. Cells were incubated with MTT solution at 0.5 mg $mL^{-1}$ MTT final concentration for up to 4 h. Media was then removed and the formazan produced was dissolved in 200 μL DMSO and absorbance was read in a plate reader at 560 nm.

*Tumor xenograft implantation and animal survival studies:* All animal experiments were performed in compliance with the UK Home Office Code of Practice for the Housing and Care of Animals Used in Scientific Procedures. Six-to-eight-week-old female CD1 nude mice (Charles River Laboratories, UK) were caged in individually vented cages (IVC; Allentown, USA) in groups of four to six animals with free access to food and water. A temperature of 19–22 °C was maintained, with a relative humidity of 45–65%, and a 12 h light/dark cycle. Mice were inoculated subcutaneously with $1 \times 10^6$ Calu 6 human epithelial lung carcinoma cells mixed 1:1 with Matrigel (Becton Dickinson, UK) in 100 μL on the left flank. The tumor volume was estimated by bilateral Vernier caliper measurement three to four times per week and calculated using the formula (width × width) × (length) × ($\pi$/6), where length was taken to be the longest diameter across the tumor, as previously described.[37] Intratumoral injections were performed when the tumor volume reached 200–400 $mm^3$.

For intratumoral administration and tissue analysis, mice were anesthetized using isofluorane and injected with the siRNA alone or the complex prepared in 5% dextrose. The needle was inserted in the longitudinal direction from the tumor edge into the center of the tumor, 50 μL of the dispersion was administered slowly over 1 min, and the needle was left in the tumor for another 5 min to prevent sample leakage. Injections were carried out on days 14, 20, 24, 31, and 38 following tumor inoculation. Mice were sacrificed by cervical dislocation when tumor volume reached 800–1000 $mm^3$.

*Heamatoxylin/eosin (H&E) tissue histology:* For histological analysis, tumors, lung, liver, spleen, and kidneys were fixed in 10% buffered formalin and processed for routine histology with hematoxylin and eosin stain by the Laboratory Diagnostic Service of the Royal Veterinary College (London, UK). Microscopic observation of tissues was carried out with Nikon Microphot-FXA microscope coupled with Infinity 2 digital camera.

*TUNEL/PI assay:* Tissue sections were deparaffinized in Histoclear and rehydrated through graded ethanol. The Dead-EndFluorometric TUNEL System (Promega, UK) was used to label nicked DNA through incorporation of fluorescein-12-dUTP. Samples were incubated with recombinant Terminal Deoxynucleotidyl Transferase (rTdT) as per manufacturer's instructions and fluorescein labelling was visualized using confocal microscopy (LSM 510, Zeiss UK). Propidium iodide was used to counterstain nuclei.

*Statistical analysis:* Data was expressed as mean ± s.e.m. where indicated. Statistical differences were analysed using the Student's t-test and p values $<0.05$ were taken to be statistically significant.

## Acknowledgements

*J.E.P. is the recipient of a CASE Award Ph.D. studentship from the Biotechnology and Biological Sciences Research Council (UK) in collaboration with AstraZeneca plc. Dr. R. Odedra and Dr. A. Ryan at AstraZeneca plc are acknowledged for assistance with establishment of the human xenograft model. H.A.B. acknowledges the Ministére de l'Enseignement Supèrieur et de la Recherche Scientifique (Algeria) for a full Ph.D. scholarship. M.A.H. acknowledges support by the Junta de Comunidades de Castilla la Mancha (Spain) for the award of a post-doctoral fellowship. A.B. acknowledges support by the CNRS and the Agence Nationale de la Recherche (grant ANR-05-JCJC-0031-01). M.P. acknowledges the University of Trieste, Regione Friuli-Venezia Giulia and MUR (PRIN 2006, prot. 2006034372). The work is partly supported by the European Union FP6 NEURONANO (NMP4-CT-2006-031847) and NINIVE (NMP4-CT-2006-033378) research programmes.*

[1] A. Fire, S. Xu, M. K. Montgomery, S. A. Kostas, S. E. Driver, C. C. Mello, *Nature* **1998**, *391*, 806.
[2] S. M. Elbashir, J. Harborth, W. Lendeckel, A. Yalcin, K. Weber, T. Tuschl, *Nature* **2001**, *411*, 494.
[3] A. de Fougerolles, H. P. Vornlocher, J. Maraganore, J. Lieberman, *Nat. Rev. Drug. Discov.* **2007**, *6*, 443.
[4] G. Meister, T. Tuschl, *Nature* **2004**, *431*, 343.
[5] P. Y. Lu, M. C. Woodle, *Methods Mol. Biol.* **2008**, *437*, 93.
[6] T. Nguyen, E. M. Menocal, J. Harborth, J. H. Fruehauf, *Curr. Opin. Mol. Ther.* **2008**, *10*, 158.
[7] A. Akinc, A. Zumbuehl, M. Goldberg, E. S. Leshchiner, V. Busini, N. Hossain, S. A. Bacallado, D. N. Nguyen, J. Fuller, R. Alvarez, A. Borodovsky, T. Borland, R. Constien, A. de Fougerolles, J. R. Dorkin, K. Narayanannair Jayaprakash, M. Jayaraman, M. John, V. Koteliansky, M. Manoharan, L. Nechev, J. Qin, T. Racie, D. Raitcheva, K. G. Rajeev, D. W. Sah, J. Soutschek, I. Toudjarska, H. P. Vornlocher, T. S. Zimmermann, R. Langer, D. G. Anderson, *Nat. Biotechnol.* **2008**, *26*, 561.
[8] D. W. Bartlett, H. Su, I. J. Hildebrandt, W. A. Weber, M. E. Davis, *Proc. Natl. Acad. Sci. U S A* **2007**, *104*, 15549.
[9] D. L. Lewis, J. A. Wolff, *Adv. Drug Deliv. Rev.* **2007**, *59*, 115.
[10] T. S. Zimmermann, A. C. Lee, A. Akinc, B. Bramlage, D. Bumcrot, M. N. Fedoruk, J. Harborth, J. A. Heyes, L. B. Jeffs, M. John, A. D. Judge, K. Lam, K. McClintock, L. V. Nechev, L. R. Palmer, T. Racie, I. Rohl, S. Seiffert, S. Shanmugam, V. Sood, J. Soutschek, I. Toudjarska, A. J. Wheat, E. Yaworski, W. Zedalis, V. Koteliansky, M. Manoharan, H. P. Vornlocher, I. MacLachlan, *Nature* **2006**, *441*, 111.

  

[11] J. D. Heidel, Z. Yu, J. Y. Liu, S. M. Rele, Y. Liang, R. K. Zeidan, D. J. Kornbrust, M. E. Davis, *Proc. Natl. Acad. Sci. U S A* **2007**, *104*, 5715.
[12] C. Huang, M. Li, C. Chen, Q. Yao, *Expert Opin. Ther. Targets* **2008**, *12*, 637.
[13] K. F. Pirollo, E. H. Chang, *Cancer Res.* **2008**, *68*, 1247.
[14] J. Yano, K. Hirabayashi, S. Nakagawa, T. Yamaguchi, M. Nogawa, I. Kashimori, H. Naito, H. Kitagawa, K. Ishiyama, T. Ohgi, T. Irimura, *Clin. Cancer Res.* **2004**, *10*, 7721.
[15] T. G. Liu, J. Q. Yin, B. Y. Shang, Z. Min, H. W. He, J. M. Jiang, F. Chen, Y. S. Zhen, R. G. Shao, *Cancer Gene Ther.* **2004**, *11*, 748.
[16] M. Nogawa, T. Yuasa, S. Kimura, M. Tanaka, J. Kuroda, K. Sato, A. Yokota, H. Segawa, Y. Toda, S. Kageyama, T. Yoshiki, Y. Okada, T. Maekawa, *J. Clin. Invest.* **2005**, *115*, 978.
[17] S. D. Li, S. Chono, L. Huang, *Mol. Ther.* **2008**, *16*, 942.
[18] K. F. Pirollo, A. Rait, Q. Zhou, S. H. Hwang, J. A. Dagata, G. Zon, R. I. Hogrefe, G. Palchik, E. H. Chang, *Cancer Res.* **2007**, *67*, 2938.
[19] A. Santel, M. Aleku, O. Keil, J. Endruschat, V. Esche, B. Durieux, K. Loffler, M. Fechtner, T. Rohl, G. Fisch, S. Dames, W. Arnold, K. Giese, A. Klippel, J. Kaufmann, *Gene Ther.* **2006**, *13*, 1360.
[20] A. Santel, M. Aleku, O. Keil, J. Endruschat, V. Esche, G. Fisch, S. Dames, K. Loffler, M. Fechtner, W. Arnold, K. Giese, A. Klippel, J. Kaufmann, *Gene Ther.* **2006**, *13*, 1222.
[21] K. Iwaki, K. Shibata, M. Ohta, Y. Endo, H. Uchida, M. Tominaga, R. Okunaga, S. Kai, S. Kitano, *Int. J. Cancer* **2008**, *122*, 658.
[22] K. Futami, E. Kumagai, H. Makino, A. Sato, M. Takagi, A. Shimamoto, Y. Furuichi, *Cancer Sci.* **2008**, *99*, 1227.
[23] Q. Leng, P. Scaria, P. Lu, M. C. Woodle, A. J. Mixson, *Cancer Gene Ther.* **2008**.
[24] R. M. Schiffelers, A. Ansari, J. Xu, Q. Zhou, Q. Tang, G. Storm, G. Molema, P. Y. Lu, P. V. Scaria, M. C. Woodle, *Nucleic Acids Res.* **2004**, *32*, e149.
[25] B. Urban-Klein, S. Werth, S. Abuharbeid, F. Czubayko, A. Aigner, *Gene Ther.* **2005**, *12*, 461.
[26] D. Pantarotto, R. Singh, D. McCarthy, M. Erhardt, J. P. Briand, M. Prato, K. Kostarelos, A. Bianco, *Angew. Chem. Int. Ed.* **2004**, *43*, 5242.
[27] R. Singh, D. Pantarotto, L. Lacerda, G. Pastorin, C. Klumpp, M. Prato, A. Bianco, K. Kostarelos, *Proc. Natl. Acad. Sci. USA* **2006**, *103*, 3357.
[28] K. Kostarelos, L. Lacerda, G. Pastorin, W. Wu, S. Wieckowski, J. Luangsivilay, S. Godefroy, D. Pantarotto, J.-P. Briand, S. Muller, M. Prato, A. Bianco, *Nat. Nano.* **2007**, *2*, 108.
[29] N. W. Kam, Z. Liu, H. Dai, *J. Am. Chem. Soc.* **2005**, *127*, 12492.
[30] Z. Liu, M. Winters, M. Holodniy, H. Dai, *Angew. Chem. Int. Ed.* **2007**, *46*, **2023**.
[31] R. Krajcik, A. Jung, A. Hirsch, W. Neuhuber, O. Zolk, *Biochem. Biophys. Res. Commun.* **2008**, *369*, 595.
[32] X. Wang, J. Ren, X. Qu, *ChemMedChem* **2008**, *3*, 940.
[33] Z. Zhang, X. Yang, Y. Zhang, B. Zeng, S. Wang, T. Zhu, R. B. Roden, Y. Chen, R. Yang, *Clin. Cancer Res.* **2006**, *12*, 4933.
[34] B. T. Martin, K. Strebhardt, *Cell Cycle* **2006**, *5*, 2881.
[35] A. Casey, E. Herzog, M. Davoren, F. M. Lyng, H. J. Byrne, G. Chambers, *Carbon* **2007**, *45*, 1425.
[36] J. M. Worle-Knirsch, K. Pulskamp, H. F. Krug, *Nano Lett.* **2006**, *6*, 1261.
[37] S. R. Wedge, J. Kendrew, L. F. Hennequin, P. J. Valentine, S. T. Barry, S. R. Brave, N. R. Smith, N. H. James, M. Dukes, J. O. Curwen, R. Chester, J. A. Jackson, S. J. Boffey, L. L. Kilburn, S. Barnett, G. H. Richmond, P. F. Wadsworth, M. Walker, A. L. Bigley, S. T. Taylor, L. Cooper, S. Beck, J. M. Jurgensmeier, D. J. Ogilvie, *Cancer Res.* **2005**, *65*, 4389.
[38] L. Lacerda, S. Raffa, M. Prato, A. Bianco, K. Kostarelos, *Nano Today* **2007**, *2*, 38.
[39] S. Dow, *Expert Opin. Drug Deliv.* **2008**, *5*, 11.
[40] P. P. Karmali, A. Chaudhuri, *Med. Res. Rev.* **2007**, *27*, 696.
[41] A. Aigner, *Curr. Opin. Mol. Ther.* **2007**, *9*, 345.
[42] S. Zhang, B. Zhao, H. Jiang, B. Wang, B. Ma, *J. Controlled Release.* **2007**, *123*, 1.
[43] I. Ito, L. Ji, F. Tanaka, Y. Saito, B. Gopalan, C. D. Branch, K. Xu, E. N. Atkinson, B. N. Bekele, L. C. Stephens, J. D. Minna, J. A. Roth, R. Ramesh, *Cancer Gene Ther.* **2004**, *11*, 733.
[44] R. Ramesh, T. Saeki, N. S. Templeton, L. Ji, L. C. Stephens, I. Ito, D. R. Wilson, Z. Wu, C. D. Branch, J. D. Minna, J. A. Roth, *Mol. Ther.* **2001**, *3*, 337.
[45] C. M. Wiethoff, J. G. Koe, G. S. Koe, C. R. Middaugh, *J. Pharm. Sci.* **2004**, *93*, 108.
[46] W. Yeeprae, S. Kawakami, S. Suzuki, F. Yamashita, M. Hashida, *Pharmazie* **2006**, *61*, 102.
[47] L. Zender, S. Kubicka, *Apoptosis* **2004**, *9*, 51.
[48] S. Ray, A. Almasan, *Cancer Res.* **2003**, *63*, 4713.
[49] A. Verma, S. Guha, P. Diagaradjane, A. B. Kunnumakkara, A. M. Sanguino, G. Lopez-Berestein, A. K. Sood, B. B. Aggarwal, S. Krishnan, J. G. Gelovani, K. Mehta, *Clin. Cancer Res.* **2008**, *14*, 2476.
[50] P. Yadava, D. Roura, J. A. Hughes, *Oligonucleotides* **2007**, *17*, 213.
[51] B. R. Davies, A. Logie, J. S. McKay, P. Martin, S. Steele, R. Jenkins, M. Cockerill, S. Cartlidge, P. D. Smith, *Mol. Cancer. Ther.* **2007**, *6*, 2209.
[52] L. Lacerda, A. Bianco, M. Prato, K. Kostarelos, *J. Mat. Chem.* **2008**, *18*, 17.
[53] B. Kateb, M. Van Handel, L. Zhang, M. J. Bronikowski, H. Manohara, B. Badie, *Neuroimage* **2007**, *37* Suppl 1, S9.
[54] B. Shekunov, *IDrugs* **2005**, *8*, 399.
[55] Y. C. Tan, A. Q. Shen, Y. Li, E. Elson, L. Ma, *Lab Chip* **2008**, *8*, 339.
[56] S. E. Frew, S. M. Sammut, A. F. Shore, J. K. Ramjist, S. Al-Bader, R. Rezaie, A. S. Daar, P. A. Singer, *Nat. Biotechnol.* **2008**, *26*, 37.
[57] Q. Leng, A. J. Mixson, *Cancer Gene Ther.* **2005**, *12*, 682.
[58] Q. Leng, P. Scaria, J. Zhu, N. Ambulos, P. Campbell, A. J. Mixson, *J. Gene Med.* **2005**, *7*, 977.
[59] S. H. Kim, J. H. Jeong, S. H. Lee, S. W. Kim, T. G. Park, *J. Controlled Release* **2008**, *129*, 107.
[60] V. Georgakilas, N. Tagmatarchis, D. Pantarotto, A. Bianco, J. P. Briand, M. Prato, *Chem. Comm.* **2002**, 3050.
[61] V. Georgakilas, K. Kordatos, M. Prato, D. M. Guldi, A. M. Holzinger, A. Hirsch, *J. Am. Chem. Soc.* **2002**, *124*, 760.

Received: October 10, 2008
Revised: January 11, 2009
Published online:

  